AMERICAN SOCIETY FOR MICROBIOLOGY | Applied and Environmental Microbiology®

METHODS

Portable CRISPR-Cas9^N System for Flexible Genome Engineering in *Lactobacillus acidophilus*, *Lactobacillus gasseri*, and *Lactobacillus paracasei*

Yong Jun Goh,[a] **Rodolphe Barrangou**[a]

[a]Department of Food, Bioprocessing and Nutrition Sciences, North Carolina State University, Raleigh, North Carolina, USA

ABSTRACT Diverse *Lactobacillus* strains are widely used as probiotic cultures in the dairy and dietary supplement industries, and specific strains, such as *Lactobacillus acidophilus* NCFM, have been engineered for the development of biotherapeutics. To expand the *Lactobacillus* manipulation toolbox with enhanced efficiency and ease, we present here a CRISPR (clustered regularly interspaced palindromic repeats)-SpyCas9^{D10A} nickase (Cas9^N)-based system for programmable engineering of *L. acidophilus* NCFM, a model probiotic bacterium. Successful single-plasmid delivery system was achieved with the engineered pLbCas9^N vector harboring *cas9*^{N} under the regulation of a *Lactobacillus* promoter and a cloning region for a customized single guide RNA (sgRNA) and editing template. The functionality of the pLbCas9^N system was validated in NCFM with targeted chromosomal deletions ranging between 300 bp and 1.9 kb at various loci (*rafE*, *lacS*, and *ltaS*), yielding 35 to 100% mutant recovery rates. Genome analysis of the mutants confirmed precision and specificity of the pLbCas9^N system. To showcase the versatility of this system, we also inserted an mCherry fluorescent-protein gene downstream of the *pgm* gene to create a polycistronic transcript. The pLbCas9^N system was further deployed in other species to generate a concurrent single-base substitution and gene deletion in *Lactobacillus gasseri* ATCC 33323 and an in-frame gene deletion in *Lactobacillus paracasei* Lpc-37, highlighting the portability of the system in phylogenetically distant *Lactobacillus* species, where its targeting activity was not interfered with by endogenous CRISPR-Cas systems. Collectively, these editing outcomes illustrate the robustness and versatility of the pLbCas9^N system for genome manipulations in diverse lactobacilli and open new avenues for the engineering of health-promoting lactic acid bacteria.

IMPORTANCE This work describes the development of a lactobacillus CRISPR-based editing system for genome manipulations in three *Lactobacillus* species belonging to the lactic acid bacteria (LAB), which are commonly known for their long history of use in food fermentations and as indigenous members of healthy microbiotas and for their emerging roles in human and animal commercial health-promoting applications. We exploited the established CRISPR-SpyCas9 nickase for flexible and precise genome editing applications in *Lactobacillus acidophilus* and further demonstrated the efficacy of this universal system in two distantly related *Lactobacillus* species. This versatile Cas9-based system facilitates genome engineering compared to conventional gene replacement systems and represents a valuable gene editing modality in species that do not possess native CRISPR-Cas systems. Overall, this portable tool contributes to expanding the genome editing toolbox of LAB for studying their health-promoting mechanisms and engineering of these beneficial microbes as next-generation vaccines and designer probiotics.

KEYWORDS *Lactobacillus acidophilus*, CRISPR, Cas9, nickase, genome editing, probiotic, lactic acid bacteria, *Lactobacillus*

Citation Goh YJ, Barrangou R. 2021. Portable CRISPR-Cas9^N system for flexible genome engineering in *Lactobacillus acidophilus*, *Lactobacillus gasseri*, and *Lactobacillus paracasei*. Appl Environ Microbiol 87:e02669-20. https://doi.org/10.1128/AEM.02669-20.

Editor Edward G. Dudley, The Pennsylvania State University

Address correspondence to Yong Jun Goh, yjgoh@ncsu.edu, or Rodolphe Barrangou, rbarran@ncsu.edu.

Received 29 October 2020
Accepted 10 December 2020
Accepted manuscript posted online 4 January 2021
Published 26 February 2021

Lactobacillus acidophilus is an indigenous member of the human gastrointestinal microbiota and is one of the most widely formulated probiotic strains in fermented dairy products, functional foods, and dietary supplements (1). A member of the phylum *Firmicutes*, *L. acidophilus* is a monophyletic Gram-positive lactic acid bacterial species (2) that is a facultative anaerobe, non-spore-forming, and homofermentative. The model strain *L. acidophilus* NCFM is a human isolate which has been broadly commercialized since the 1970s (3). The health-promoting attributes of NCFM have been well documented, such as the reduction of cold- and flu-like symptom incidence and duration in children and the modulation of intestinal visceral pain receptors and immune cell functions (4–6). The intrinsic ability of *L. acidophilus* NCFM to survive gut passage, in combination with its amenability to industrial production and genetic manipulations, has sparked interest in developing this strain into designer probiotics with enhanced functionality, and it constitutes an ideal chassis for oral delivery of mucosal vaccines and biotherapeutics (7, 8). Efforts under way to further elucidate the molecular mechanisms involved in the health-promoting effects of *L. acidophilus* also hinge on efficient molecular tools that enable genetic manipulation to decipher gene functions responsible for health-promoting attributes.

The first-generation genome manipulation system in *L. acidophilus* was based on single-crossover homologous recombination driven by conditional plasmid replication to generate targeted gene knockouts (9, 10). This system relied on the concurrent use of a broad-host-range nonreplicative pWV01-derived vector (Ori^+ $RepA^-$) carrying a gene fragment homologous to the target deletion and a temperature-sensitive helper plasmid, pTRK669, which provides *repA* in *trans* for conditional replication of the pORI-based plasmids. A markerless gene replacement system with *upp*-based counterselection was subsequently developed which has drastically increased the efficiency for generating single and multiple chromosomal deletions and gene insertions by providing direct selection for double-crossover recombinants (11, 12). Nonetheless, despite the convenience of efficient counterselection, the gene replacement procedures typically take a minimum of 2 weeks after plasmid transformation for single- and double-crossover event selections. In addition, the *upp*-based system requires prior establishment of an isogenic *upp*-null mutant as a background host to confer resistance against the 5-fluorouracil counterselective agent.

The discovery and characterization of prokaryotic CRISPR-Cas (clustered regularly interspaced short palindromic repeats–CRISPR-associated protein)-adaptive immune systems and the subsequent repurposing of Cas effectors for genome editing have revolutionized biology and genetics in the past decade (13–22). CRISPR-Cas systems confer adaptive immunity in prokaryotes against phages and foreign genetic elements, as well as other biological functions beyond immunity (23, 24). The sequence-specific targeting of nucleic acids via RNA-guided CRISPR-associated (Cas) effector proteins presents unique opportunities for repurposing these molecular machines into programmable genome editing tools (15). In particular, the popular Cas9 endonuclease from the *Streptococcus pyogenes* (SpyCas9) class 2 type II CRISPR-Cas system can be codelivered with a target-specific chimeric single guide RNA (sgRNA) to drive precise double-stranded-DNA cleavage (15). The portability of the Cas9 single effector protein provides convenience for heterologous expression in a wide range of hosts along with a customized homing "spacer" sequence in the sgRNA to guide Cas9 cleavage to the complementary protospacer adjacent to Cas9-specific sequence recognition, termed the protospacer-adjacent motif (PAM), in the host chromosome (17, 25–27). Precise deletions, insertions, or point mutations can be readily achieved by codelivering a DNA template that serves as a repair template to guide and budge the host DNA repair pathways (18, 26–29). Implementation of CRISPR-Cas editing in prokaryotes has gradually gained more traction, with CRISPR-based editing tool kits recently having been developed for *Escherichia coli* (27, 30–32), *Bacillus* (33–35), *Lactococcus lactis* (36), *Clostridium* (37, 38), *Corynebacterium* (39), and actinomycetes (40–42) (reviewed in reference 43). Nickase variants of SpyCas9 with inactivated RuvC ($Cas9^{D10A}$) or HNH

(Cas9^{H840A}) nuclease domain were developed for genome editing, which results in single-stranded incision at the target DNA, thus greatly improving editing efficiencies in bacteria that lack efficient pathways to repair double-stranded-DNA breaks (15–17, 32, 34, 35, 38).

The potential of CRISPR-SpyCas9-based genome editing was recently reported for several *Lactobacillus* species. In *Lactobacillus reuteri*, the use of CRISPR-Cas9 coupled with recombinase T (RecT)-mediated single-stranded DNA (ssDNA) oligonucleotide recombineering provided high-efficiency selection of edited cells for oligonucleotide-mediated chromosomal deletions up to a 1-kb region (44). A similar approach using Cas9-based RecT-assisted ssDNA recombineering was compared with plasmid-borne recombineering template to perform point mutations in three different *Lactobacillus plantarum* strains (45). The comparison revealed variability in editing efficiencies based on strains and methods of repair template delivery. More recently, Zhou et al. (46) employed Cas9/RecT-assisted ssDNA recombineering in combination with host-derived DNA adenine methylase to improve the efficiency of ssDNA recombineering-mediated point mutations in *L. plantarum*. Gene deletion was further approached with Cas9/RecT-assisted double-stranded DNA (dsDNA) recombineering, in conjunction with the coexpression of host prophage-derived exonuclease analog and a putative host-nuclease inhibitor to improve homologous recombination of the dsDNA template and host chromosome. To enhance editing efficiency, the dsDNA template was protected from cytoplasmic exonuclease degradation by the incorporation of phosphorothioate bonds (46). To overcome the toxicity of Cas9-induced double-stranded breaks, Song et al. (47) achieved efficient gene deletion and insertion in *Lactobacillus casei* using a Cas9^{D10A} nickase variant in combination with target-specific sgRNA and plasmid-borne repair templates. In strains of *L. plantarum* and *Lactobacillus brevis* with inefficient homology-directed repair (HDR), even with nonlethal Cas9 nickase-induced nicks, Huang et al. (48) combined the host-derived prophage recombinases RecE and RecT with the native Cas9 to achieve efficient gene deletions and gene replacement.

As a genetically and functionally diverse group of widespread species, the genus *Lactobacillus* is enriched with CRISPR-Cas immune systems (49). For species that possess functional CRISPR-Cas systems (for example, *Lactobacillus crispatus*), the endogenous type I-E CRISPR-Cas system can be hijacked for genome editing with plasmid delivery of customized gRNA and repair templates that coopt and redirect the immune system toward self and drive efficient genome editing (50). On the other hand, species and strains lacking functional CRISPR-Cas systems, such as *L. acidophilus*, need the deployment of plasmid-encoded portable effectors for genome editing (49, 51). CRISPR-based genome editing in this species and others lacking intact CRISPR-Cas systems will require heterologous CRISPR and Cas expression systems. Here, we report the development of a *Lactobacillus* SpyCas9-based genome editing tool kit for programmable editing in *L. acidophilus*, which can also be widely applicable to other health-promoting and industry-relevant *Lactobacillus* species. Due to the general lack of robust DNA repair mechanisms, such as nonhomologous-end-joining (NHEJ) DNA repair pathway in *Lactobacillus*, we exploited the established Cas9^{D10A} nickase variant (Cas9^{N}) for targeted gene deletion and insertion in *L. acidophilus* to circumvent double-strand-break-induced lethality. The portability of the resulting pLbCas9^{N} system was further demonstrated in two phylogenetically distant species, *Lactobacillus gasseri* and *Lactobacillus paracasei*. The high editing efficiency of the pLbCas9^{N} system in *L. paracasei* indicates that the heterologous CRISPR-Cas9^{N} targeting activity was not interfered with by the host's endogenous type I-E CRISPR-Cas system, highlighting applications of the pLbCas9^{N} system beyond species devoid of native CRISPR-Cas systems.

RESULTS AND DISCUSSION

Establishment of a CRISPR-SpyCas9^{D10A} nickase (Cas9^{N}) system in *L. acidophilus* NCFM. The Cas9^{N}-sgRNA genome editing system for *L. acidophilus* is composed of a Gram-positive-*E. coli* shuttle vector system harboring *cas9*^{N} under the regulation of the P6 *Lactobacillus* promoter, sgRNA driven by the endogenous promoter of elongation

TABLE 1 Bacterial strains and plasmids used in this study

Strain or plasmid	Genotype or characteristic	Source or reference
Strains		
L. acidophilus		
NCK56	NCFM strain, human intestinal isolate	79
NCK2773	NCFM carrying a 300-bp in-frame deletion within *rafE*	This study
NCK2774	NCFM carrying a 1,086-bp in-frame deletion within *lacS*	This study
NCK2676	NCFM carrying a 1,919-bp deletion within *ltaS*	This study
NCK2777	NCFM with 731-bp mCherry gene translational cassette inserted downstream of *pgm*	This study
L. gasseri		
NCK334	ATCC 33323 strain, human isolate, type strain	ATCC
NCK2775	ATCC 33323 carrying a premature stop codon and a 562-bp deletion within *2crr* (LGAS_0710)	This study
L. paracasei		
NCK2639	Lpc-37 (ATCC SD5275) Florafit strain, isolated from a dairy source	DuPont
NCK2776	Lpc-37 carrying a 1,299-bp in-frame deletion within *glgA* (LPC37PB_RS04825)	This study
E. coli		
MC1061	Cloning host, Str^r	80
Plasmids		
pTRK687	3.018 kb; pNZ-based shuttle vector derivative, contains P6 promoter, Cm^r	54
pTRK1203	pLbCas9^N; 7.149 kb; pTRK687 with SpyCas9^{D10A} gene cloned downstream of P6 promoter	This study
pTRK1248	7.566 kb; pTRK1203 containing NCK56 P*tuf*-sgRNA for *rafE* targeting	This study
pTRK1204	9.568 kb; pTRK1203 containing NCK56 P*tuf*-sgRNA-editing template for Δ*rafE*	This study
pTRK1249	7.566 kb; pTRK1203 containing NCK56 P*tuf*-sgRNA for *lacS* targeting	This study
pTRK1205	9.591 kb; pTRK1203 containing NCK56 P*tuf*-sgRNA-editing template for Δ*lacS*	This study
pTRK1254	9.604 kb; pTRK1203 containing NCK56 P*tuf*-sgRNA-editing template for Δ*ltaS*	This study
pTRK1255	11.374 kb; pTRK1203 containing NCK56 P*tuf*-sgRNA-editing template for mCherry gene insertion	This study
pTRK1256	9.235 kb; pTRK1203 containing NCK334 P*tuf*-sgRNA-editing template for Δ*2crr*	This study
pTRK1257	9.586 kb; pTRK1203 containing NCK2639 P*tuf*-sgRNA-editing template for Δ*glgA*	This study

factor-Tu gene (*tuf*), an editing template consisting of 1-kb homologous arms flanking the editing site, and a chloramphenicol (Cm) selection marker. Preliminary strategies for developing a Cas9^N genome editing system entailed either delivering the Cas9^N and target-specific sgRNA in tandem with the repair template in a single-plasmid system or delivering the latter two components on separate plasmids in a two-plasmid delivery system in order to minimize the size of vector constructs. For both single- and two-plasmid-system approaches, delivery of Cas9^N based on the Gram-positive-*E. coli* shuttle plasmid pGK12 (52) was unsuccessful due to instability of the *cas9*^{N} expression cassette in various *E. coli* cloning hosts tested, as well as in *L. acidophilus*. Subsequently, successful construction of the Cas9^N expression plasmid was achieved in a Gram-positive broad-host-range pNZ-based plasmid (53), pTRK687 (54). Expression of Cas9^N is driven by the P6 promoter, an established high-expression promoter in lactobacilli (55), with restriction sites located downstream of the P6-*cas9*^{N} cassette for cloning of sgRNA and homologous editing templates. The resulting 7.1-kb Cas9^N vector, designated pLbCas9^N (pTRK1203) (Table 1), is stable in selecting *E. coli* cloning hosts and was transformable into *L. acidophilus* NCFM with relatively high efficiency at $\geq 2 \times 10^3$ CFU/μg of vector DNA. To confirm the stability of the *cas9*^{N} insert in NCFM, total DNA was extracted from two selected pLbCas9^N transformants for PCR amplification of *cas9*^{N}. Sequencing of the PCR amplicons confirmed intact *cas9*^{N} in both transformants, verifying the fidelity of pLbCas9^N replication in *L. acidophilus*.

Gene deletions in *L. acidophilus* using the pLbCas9^N system. To evaluate the functionality of the pLbCas9^N system in *L. acidophilus* NCFM, three targeted chromosomal deletions of various sizes were performed within the (i) raffinose ABC transporter substrate-binding protein gene *rafE* (deletion of 300 bp), (ii) lactose permease gene *lacS* (deletion of 1,086 bp), and (iii) phosphoglycerol transferase gene *ltaS* (deletion of 1,919 bp) of the lipoteichoic acid biosynthesis pathway (Fig. 1). Each editing construct consisted of the NCFM *tuf* promoter (P*tuf*) upstream of a target-specific sgRNA along with the editing template, the latter composed of 1-kb homologous regions flanking

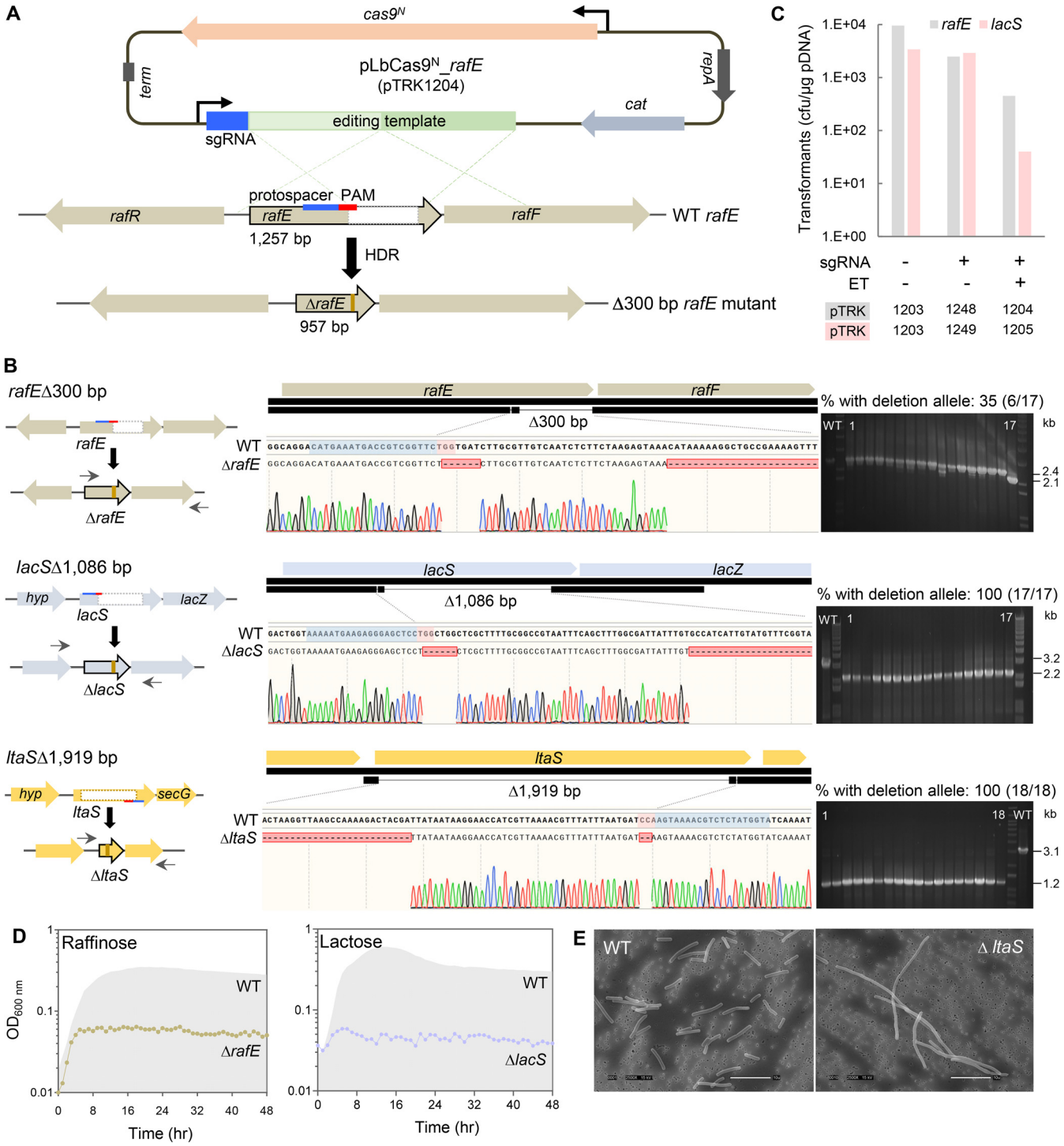

FIG 1 Heterologous expression of Cas9^N and sgRNA via the pLbCas9^N system for CRISPR-guided gene deletions in *L. acidophilus* NCFM. (A) Schematic overview of constructing a 300-bp in-frame deletion within the *rafE* gene. Target-specific sgRNA and an editing template consisting of 1-kb DNA fragments homologous to the regions flanking the target deletion were cloned into the pLbCas9^N vector. Expression of Cas9^N and sgRNA encoded in the generated plasmid, pLbCas9^N*_rafE* (pTRK1204), resulted in a single nick cleavage at the targeted site within *rafE*. Homology-directed repair (HDR) of the DNA nick by the host, assisted by the editing template in pLbCas9^N*_rafE*, leads to precise in-frame deletion at the target site in the *rafE* mutant. (B and C) Gene deletions of various sizes and in different genomic loci using the pLbCas9^N system and transformation efficiencies of the *rafE* and *lacS* editing and control plasmid variants. Cells were transformed with pLbCas9^N plasmids (pTRK1203 to -1205 and pTRK1248 and -1249) (Table 1) with and without target-specific sgRNA and editing templates (ET) for HDR. Cas9^N-targeted single-nick cleavage did not significantly affect transformation efficiencies (sgRNA+, ET−), indicating that Cas9^N expression was atoxic and cells were capable of DNA repair to overcome Cas9^N cleavage with the provision of homologous editing templates. Sanger sequencing of the PCR amplicons verified the precise deletion genotype profiles, along with the targeted PAM removal (and several bases downstream of PAM to create in-frame deletions for *rafE* and *lacS*). A 30- to 40-bp short homologous region downstream of the PAM prior to the targeted deletion regions was also included in the editing template, to ensure adequate homologous regions adjacent to the incision site for host's HDR

(Continued on next page)

the targeted site as a repair template (Fig. 1A). The repair templates were customized such that a portion of the PAM was removed in the repair template to circumvent subsequent Cas9^N cleavage once editing took place in cells with the mutated allele (Fig. 1B). In the case of *rafE* and *lacS* deletions, several bases downstream of the PAM were also removed to create in-frame deletions. In order to ensure that adequate homologous regions adjacent to the Cas9^N incision site was provided for the host's HDR pathway, the repair templates also included a 30- to 40-bp short homologous region downstream of the PAM site prior to the targeted deletion regions. The selected gRNAs for both *rafE* and *lacS* loci targeted the noncoding strand, whereas the gRNA for *ltaS* was designed to target the coding strand (Fig. 1B), with the single nick by Cas9^{D10A} occurring at the corresponding targeted strands.

Each editing construct was cloned into pLbCas9^N downstream of *cas9*^{N}, resulting in pTRK1204 (*rafE*) (Fig. 1A), pTRK1205 (*lacS*), and pTRK1254 (*ltaS*) CRISPR-editing plasmids (Table 1). Transformation efficiencies for the editing plasmids targeting *rafE*, *lacS*, and *ltaS* were 1.3 log (Fig. 1C), 1.9 log (Fig. 1C), and 1.1 log lower than that for the pLbCas9^N control vector. For both transformation experiments targeting *rafE* and *lacS*, cells were transformed with pLbCas9^N plasmids with and without target-specific sgRNA and editing templates for HDR (Fig. 1C). Cas9^N-targeted single-nick cleavage did not significantly affect transformation efficiencies (Fig. 1C, sgRNA+ ET− [pTRK1248 and pTRK1249]), indicating that Cas9^N expression was atoxic. Cells were capable of DNA repair to overcome Cas9^N cleavage with the provision of homologous editing templates (Fig. 1C, sgRNA+ ET+ [pTRK1204 and pTRK1205]), although the lower transformation efficiencies observed with pLbCas9^N editing plasmids containing both sgRNA and editing template could be attributed to the larger size of the editing plasmids (Table 1). Colony PCR screening of randomly selected transformants with chromosomal-specific primers flanking the deletion targets revealed the presence of deletion alleles in 35% (6/17), 100% (33/33), and 100% (41/41) of *rafE*, *lacS*, and *ltaS* loci, respectively (Fig. 1B). The observed high editing efficiencies for *lacS* and *ltaS* indicated effective expression of both *cas9*^{N} and sgRNA and the absence of Cas9^N toxicity. In addition, *L. acidophilus* was capable of repairing the single nick generated by Cas9^N via HDR with the concurrent provision of a homologous repair template. The lower editing efficiency observed for *rafE* deletion likely resulted from suboptimal targeting of the selected gRNA sequence. PCR screening of the pTRK1204 transformants also showed that some of the *rafE* deletion mutants were present in a mixed-genotype population. Purification of Δ*rafE* mutants was achieved by streaking and isolating pure deletion mutants on MRS medium with Cm.

Sanger sequencing of the PCR amplicons generated from the targeted sites at *rafE*, *lacS*, and *ltaS* showed precise nucleotide deletions matching the provided editing templates (Fig. 1B). The purity of each deletion mutant was further verified by PCR using one of the primers that anneal to the deletion region, where the PCR amplicon was generated only from the parent control and not the deletion mutants. For curing of the editing plasmids after successful deletion, the mutants were subcultured in MRS broth without antibiotics and plated to obtain isolated colonies. Replica plating of selected colonies on both MRS and MRS supplemented with Cm showed that 70 to 100% of the mutant colonies were Cm sensitive, indicating loss of the editing plasmids after just one passage in MRS in the absence of antibiotic selective pressure. Plasmid curing was further confirmed by the absence of PCR amplicons using primers specific for the pLbCas9^N backbone (Table 2). The efficient rate of plasmid curing enables

FIG 1 Legend (Continued)
pathway. Protospacers/guide spacer sequences and PAM are highlighted in blue and red, respectively. PCR screening of editing plasmid transformants (using the primer pairs shown on the left for respective deletion targets) revealed deletion alleles present in 35% (*rafE*, transformants 6, 7, 10, 13, 14, and 17) to 100% (*lacS* and *ltaS*, with 17 of 33 and 18 of 41 screened transformants shown, respectively) of the screened transformants. Left and right arrows represent oligonucleotide primers used for screening of deletion genotypes (Table 2). (D) Phenotypic analysis of both Δ*rafE* (NCK2773) and Δ*lacS* (NCK2774) mutants confirmed the genotypes and impaired ability of the mutants to grow on raffinose and lactose, respectively, as the sole carbon source. (E) Scanning electron microscopy imaging (magnification, ×2,500) showing that inactivation of the lipoteichoic acid biosynthetic pathway resulted in an elongated cell morphotype of the Δ*ltaS* mutant (NCK2676), which is consistent with published observations (56). Bar, 10 μm.

TABLE 2 Oligonucleotide primers used in this study

Use and oligonucleotide	Sequence (5′→3′)[a]
Amplification of *cas9*^{N}	
spycas9n-F	GTA ATA CTG CAG AAA GAG GAG AAA GGA TCT ATG GAT
spycas9n-R	TTA GTA CTG CAG TTA GTC ACC TCC TAG CTG AC
Screening of Δ*rafE* deletion	
lac_rafE-F	ATA TGT CAA AAT GTT TAT AAG GC
lac_rafE-R	TTC CAT AAT TTG CTT AGT TGT C
Screening of Δ*lacS* deletion	
lac_lacS-F	CCA AAG GAA TGC AGA GAT CG
lac_lacS-R	TGC AGG AGC ATC ATA AGT TGG
Screening of Δ*ltaS* deletion	
lac_ltaS-F	GAT TCA GGA TAA TCT TCT TCT GG
lac_ltaS-R	AAG TAA ATG TGT CTT ACT CAA TTC C
Amplification of fragments for pTRK1255 construction (mCherry gene insertion)	
lac_pgmCy-1F	AGG AGG AAC TAT ATC CGG ATG TCG AGA TCT AGA TAG TTT TGC TAG TGA TTT GG
lac_pgmCy-1R	ACT AAT TTA ATA TAG GAG ATA TTT CAT GGT TTC AAA G
lac_pgmCy-2F	GAA ATA TCT CCT ATA TTA AAT TAG TCG TCC AAC TTT TC
lac_pgmCy-2R	AGA AGG TTT TTA TAT TAC AGC TCC AGA TCT CAT CAT CTT TAT AGG TTG AAG CG
Screening of mCherry gene insertion	
lac_mCherry-F	AAT TAT CCC TGT AGC CCA CG
lac_mCherry-R	GCT GAT TTC TTT ACA CTA GCA GG
Screening of Δ2*crr* deletion	
lga_2crr-F	CAT TAT ATT TCA AGT CAT TCT TCT GC
lga_2crr-R	GGC TCA CTA GGT TTG TAC TAC
Screening of Δ*glgA* deletion	
lpc_glgA-F	TCA CGG ACC ACA TTC GTA GC
lpc_glgA-R	TGT TGT CAC CTC ATG CTT TGC
pLbCas9^N-specific primers (to verify curing of editing plasmid in mutants)	
P6-F	ATT TCT TCA CAA ATA ATT CAC GCT T
NC-R	AAT CGC TTT AGC ATC TAC TCC

[a]Restriction enzyme sites are underlined.

successive rounds of editing to generate multiple mutations in the same strain. Phenotypic analyses of the mutants confirmed the respective deletion genotypes, whereby impaired growth of both Δ*rafE* and Δ*lacS* mutants was observed when raffinose and lactose were provided as the sole carbon sources, respectively (Fig. 1D). Morphological analysis by scanning electron microscopy (SEM) of the Δ*ltaS* mutant revealed a slightly elongated cell morphotype compared to wild-type cells (Fig. 1E), which is consistent with previous observations in *L. acidophilus* mutant defective in the lipoteichoic acid biosynthetic pathway (56).

pLbCas9^N-guided chromosomal insertion in *L. acidophilus*. To further demonstrate the versatility of the pLbCas9^N system, a 711-bp gene encoding an NCFM codon-optimized mCherry fluorescent protein was targeted for chromosomal insertion immediately downstream of the *pgm* gene to create a polycistronic transcript (Fig. 2A). The assembled plasmid construct harbors an editing template consisting of an mCherry translational cassette (a native NCFM ribosomal binding site upstream of the start codon of the mCherry gene) flanked by 1.5-kb homologous arms each corresponding to the upstream and downstream regions of the insertion site. The selected protospacer and PAM were located on the minus strand, downstream of the transcriptional terminator of *pgm*. The final 11.4-kb plasmid construct, pTRK1255 (Table 1; Fig. 2A),

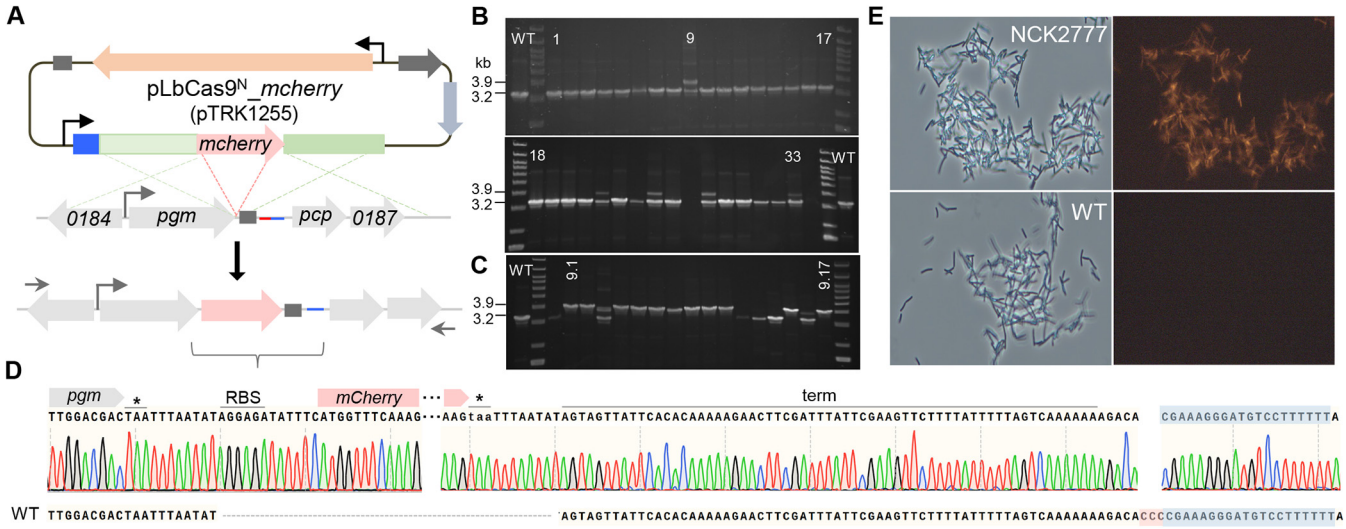

FIG 2 Chromosomal insertion of the mCherry gene in *L. acidophilus* using the pLbCas9^N system. (A) The mCherry-encoding gene was targeted for chromosomal integration downstream of *pgm* for coexpression driven by the native *pgm* promoter. The mCherry translational cassette along with 1.5-kb homologous arms and a sgRNA targeting the minus strand downstream of the transcriptional terminator (dark gray rectangles) were cloned into the pLbCas9^N vector to generate the pLbCas9^N_mCherry editing plasmid (pTRK1255). Left and right arrows represent primers used for screening of mCherry gene integrants (Table 2). (B) PCR screening of pLbCas9^N_mCherry gene transformants following subculturing steps revealed that 5/33 colonies contained mixed genotypes with the mCherry gene integrated at the targeted site (3.9-kb amplicons) in a subpopulation of the cells. (C) PCR screening of isolated colonies from transformant 9 (B) showing that the majority of the colonies are pure NCFM::mCherry gene integrants. (D) Sanger sequencing of the 3.9-kb PCR amplicon showed precise insertion of the mCherry gene cassette between *pgm* and the native transcriptional terminator (term). Asterisks indicate stop codons; the protospacer and PAM are highlighted in blue and red, respectively. Alignment with the wild-type (WT) sequence demonstrates the insertion junction and the elimination of PAM in the mCherry gene integrant. (E) Phase-contrast and fluorescence microscope examinations of the NCK2777 mCherry-expressing integrant compared to wild-type NCFM cells (magnification, ×40). mCherry fluorescence was detected in NCK2777 cells, confirming coexpression of the mCherry gene with *pgm* driven by the *pgm* promoter.

was electroporated into NCFM, with a transformation efficiency 2 log lower than that of the pLbCas9^N control vector. Initial screening of the pTRK1255 transformants did not yield any mCherry gene integrant.

To trigger continuous Cas9^N editing within the cell population and enrichment of the integrant population, the electroporated cell suspension after overnight recovery was subcultured with 0.1% inoculum for three passages in fresh MRS broth supplemented with Cm, followed by diluting and plating of the third-passage culture onto MRS medium with Cm selection. As a result of three subculturing passages, 15% (5/33) of the colonies screened contained integrant populations mixed with the wild-type genotype (Fig. 2B). One of these colonies was streaked on MRS plates with Cm to obtain isolated colonies. PCR screening of random colonies showed that 65% (11/17) were pure populations of mCherry gene integrants (Fig. 2C). PCR amplification and sequencing at the insertion site verified precise integration of the mCherry gene cassette downstream of *pgm*, prior to the transcriptional terminator (Fig. 2D). One of the integrants, designated NCK2777, was selected for the detection of mCherry fluorescent signals. Expression of mCherry proteins was confirmed by the observed fluorescent phenotype of NCK2777 under epifluorescence microscopy (Fig. 2E). Due to the general inherently low efficiencies of chromosomal gene insertion, the additional steps for enrichment of Cas9^N targeting and recovery of positive integrants demonstrated the efficacy of the pLbCas9^N system for precise gene insertion in *L. acidophilus*.

Whole-genome sequencing of *L. acidophilus* mutants confirmed target specificity of pLbCas9^N system. To verify the target specificity of the pLbCas9^N editing plasmids, the three deletion mutants from *L. acidophilus* NCFM after plasmid curing were subjected to whole-genome sequencing and sequence comparison to the wild-type NCFM genome. Mapping of the Illumina short reads from Δ*rafE*, Δ*lacS*, and Δ*ltaS* mutants against the NCFM reference genome showed the absence of sequence coverage at the targeted deletion regions in all the mutants (Fig. 3). Comparison of the assembled genomes (generated from hybrid assembly of sequences from Illumina short reads and

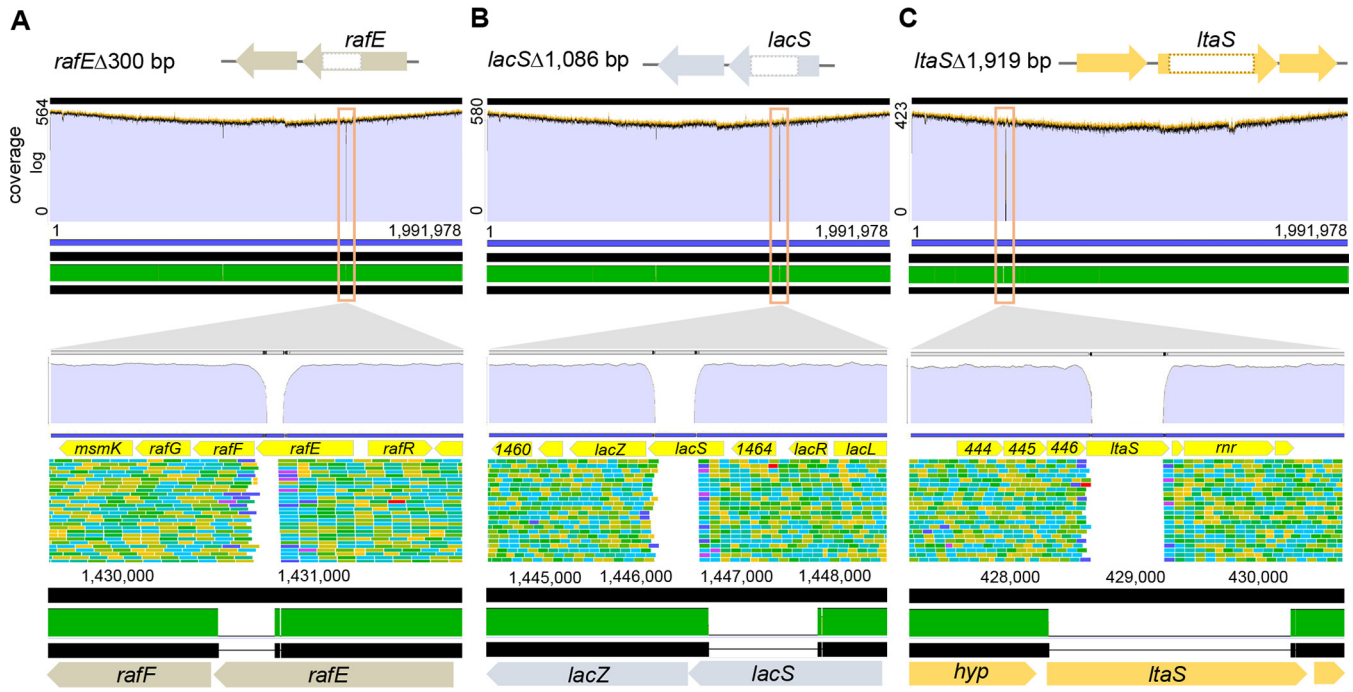

FIG 3 Whole-genome sequencing of *L. acidophilus* deletion mutants confirmed the target specificity of the pLbCas9^N-based editing plasmids for constructing deletions within (A) *rafE*, (B) *lacS*, and (C) *ltaS*, respectively, as depicted in Fig. 1. Mapping of the Illumina sequencing reads of the mutants to the parent genome (purple regions) and Mauve alignments of the whole genomes of parent and mutants (green regions) confirmed that the genome content variation (outlined by the yellow box) in each mutant is confined to the targeted deletion regions (represented by regions with no read coverage in the mutants). Bottom panels represent zoom-in visualization of the respective deletion regions within the yellow box, showing precise removal of the deletion targets.

Oxford Nanopore long reads) further confirmed the specificity of the system in achieving precise editing outcomes at all three genomic loci, with no off-targeting effects (Fig. 3). Interestingly, an insertion of a transposase gene occurred within the *lysA* gene in both the Δ*rafE* and Δ*lacS* mutants (Fig. 4A, B, and D). A closer examination of the Nanopore sequence data of the parent strain in the corresponding *lysA* region also revealed a small subpopulation of the cells with transposase-interrupted *lysA*, indicating preexisting, naturally occurring population polymorphism at this region (Fig. 4C). PCR analysis of additional Δ*rafE* and Δ*lacS* clones did not reveal transposase insertion within *lysA* (Fig. 4D). Overall, these results provide evidence that genome targeting by the pLbCas9^N editing plasmids did not trigger random transposase duplications in *L. acidophilus*.

Expansion of pLbCas9^N-mediated genome editing in *Lactobacillus paracasei* and *Lactobacillus gasseri*. The pLbCas9^N system was constructed with a pNZ-based rolling circle high-copy-number Gram-positive shuttle vector backbone that replicates in streptococci, lactococci, and lactobacilli. In addition, the constitutive P6 promoter, an *L. acidophilus* native promoter for an ArsC family transcriptional regulator designed for *cas9*^{N} expression, has also been commonly used for heterologous gene expression in other lactobacilli. To demonstrate the versatility of the pLbCas9^N system, targeted gene deletions were performed in *L. gasseri* and *L. paracasei*, two species belonging to phylogenetic clades distinct from *L. acidophilus*. *L. gasseri* strain ATCC 33323, a neotype strain of human origin and commensal of the oral, intestinal, fecal, and vaginal microbiotas of juveniles and adults (57, 58), does not have a native CRISPR-Cas system. *L. paracasei* strain Lpc-37 is a commercial probiotic strain originally isolated from a dairy source which possesses an endogenous type I-E CRISPR-Cas system. The pLbCas9^N system was used in *L. gasseri* ATCC 33323 to simultaneously generate a single base substitution to introduce a premature stop codon followed by a 562-bp deletion within the gene coding for a response regulator (2-CRR; *lgas0710*) of a two-component regulatory system (Fig. 5A). In *L. paracasei* Lpc-37, the pLbCas9^N system was designed to target an

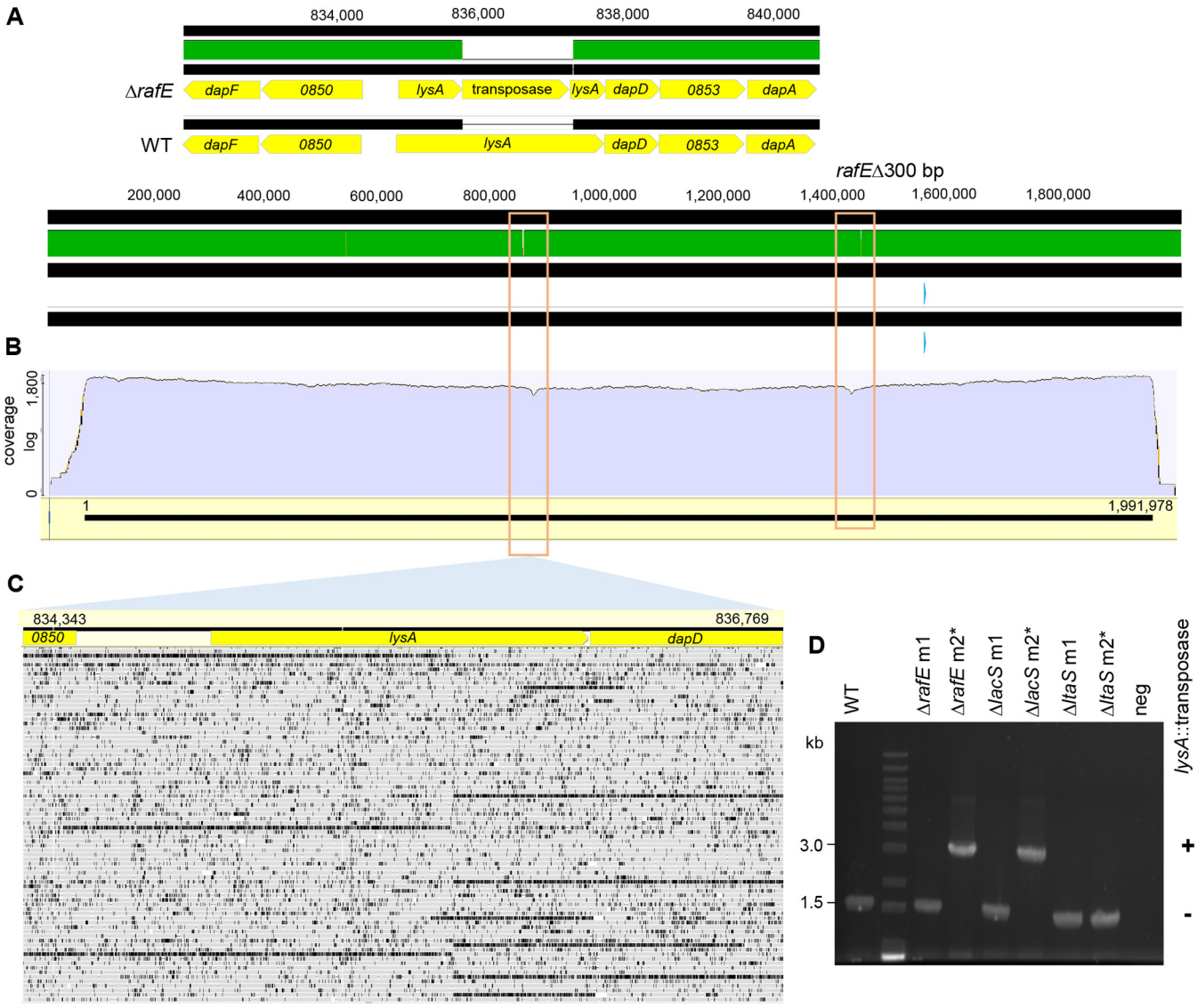

FIG 4 Detection of a spontaneous transposase gene disruption in *lysA* gene in a subpopulation of the *L. acidophilus* Δ*rafE* mutant. Whole-genome alignment (A) and mapping of Oxford Nanopore sequencing reads (B) of Δ*rafE* mutant (NCK2773) against the parent genome revealed *lysA* gene disruption by a transposase coding sequence in the mutant, a locus independent of the CRISPR-targeting *rafE* region. (C) Mapping of Oxford Nanopore sequencing reads from the parent at the corresponding region also revealed that a subset of the reads did not map contiguously to the full-length wild-type *lysA* gene, indicating spontaneous population polymorphism in this region. (D) PCR amplification of the *lysA* region in parent and all pLbCas9^N-generated mutants showed that transposase disruption within *lysA* occurred in two of the six mutant isolates (non-target specific), confirming that the observed transposase disruption is due to clonal expansion (from population polymorphism) and not to targeting by Cas9^N. Asterisks indicate mutant clones (NCK2773, NCK2774, and NCK2676) (Table 1) previously selected for genome sequencing and analysis.

in-frame deletion of 1,299 bp within the *glgA* gene, encoding a glycogen synthase of the putative glycogen biosynthesis pathway (Fig. 5B). Expression of sgRNAs was driven by the native P*tuf* promoters identified from the corresponding strains. As described previously, the customized P*tuf*-sgRNA cassette along with the 2-kb repair template (1-kb homologous regions flanking the targeted site) was cloned downstream of the P6-*cas9*^{N} expression cassette for each genome editing plasmid, generating pLbCas9^N*_2crr* (pTRK1256) and pLbCas9^N*_glgA* (pTRK1257) (Table 1).

Similar to the transformation efficiencies previously observed with the editing plasmids in *L. acidophilus*, the transformation of pTRK1256 and pTRK1257 into *L. gasseri* ATCC 33323 and *L. paracasei* Lpc-37 resulted in 1.3-log and 1.1-log reductions of transformation efficiencies in the respective strains, compared to transformation of the pLbCas9^N vector control. PCR-based screening of the transformants showed the

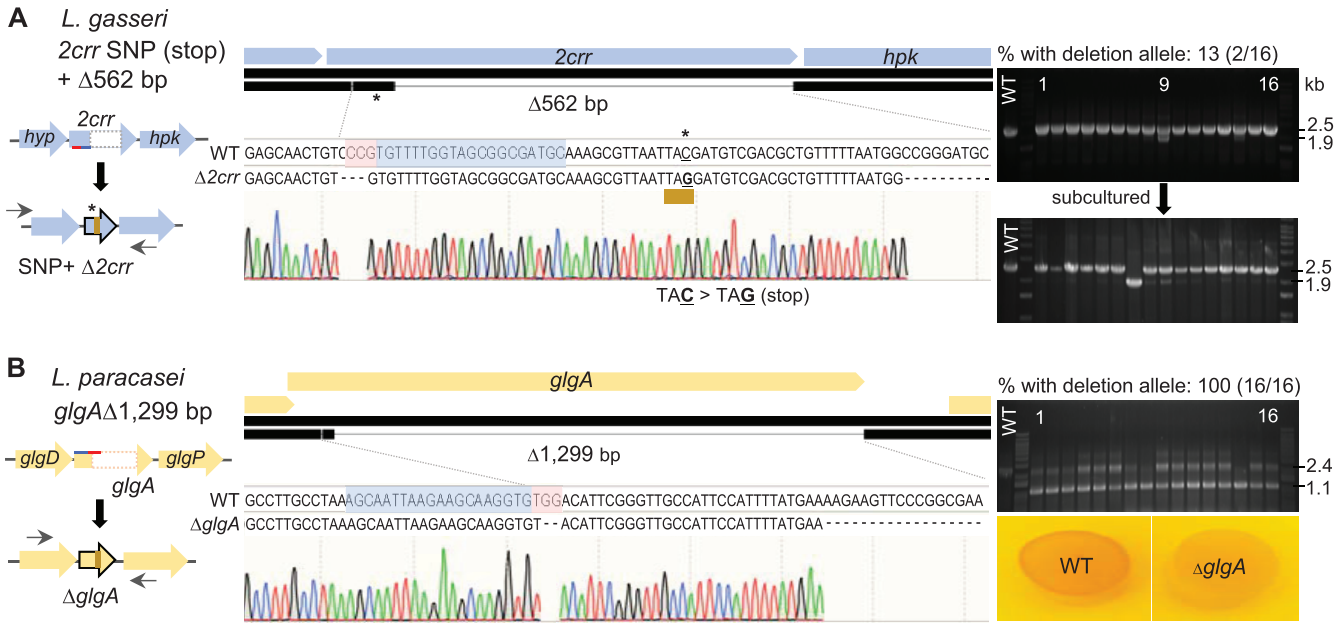

FIG 5 Portability of the pLbCas9^N system in *L. gasseri* and *L. paracasei*. (A) In *L. gasseri* ATCC 33323, the editing template cloned into pLbCas9^N was designed to create a premature stop codon by introducing a base change (C to G; indicated with an asterisk) at the 5′ region of the *2crr* gene, followed by a 562-bp deletion within the same gene. The single base change and deletion in the selected mutant (NCK2775) were confirmed by Sanger sequencing. Initial PCR screening of 16 pLbCas9^N_*2crr* (pTRK1256) transformants showed that two transformants (no. 9 and 14) contained subpopulations of cells carrying *2crr* deletion at the targeted site (1.9-kb amplicon). Subsequent PCR screening of isolated colonies from transformant 9 after subculturing in MRS with Cm yielded one pure *2crr* mutant (NCK2775) and additional colonies containing subpopulations with the *2crr* deletion. (B) For *L. paracasei* Lpc-37, the pLbCas9^N system was used to construct an in-frame deletion within the *glgA* gene. All 16 selected transformants contained the Δ*glgA* allele (1.1-kb amplicon), with the majority in mixed genotype populations containing unedited cells that can be further subcultured and purified to obtain pure mutant population. A glycogen staining assay confirmed the absence of glycogen biosynthesis in the Δ*glgA* mutant (NCK2776), as indicated by the lack of iodine staining of the mutant cells. Oligonucleotide primers used for screening deletion mutants are indicated with left and right arrows (Table 2). Blue- and red-highlighted bases represent protospacer sequences and PAM, respectively.

presence of the deletion alleles in 13% (2/16) and 100% (16/16) of the ATCC 33323 and Lpc-37 transformants, respectively (Fig. 5A and B). In both *L. gasseri* and *L. paracasei*, transformants containing mixed wild-type and mutated genotypes were easily purified by culturing in MRS supplemented with Cm to enrich for the mutated genotype and subsequent purification of the mutant population. Sequencing of PCR amplicons generated from *2crr* loci in selected ATCC 33323 mutants demonstrated precise base changes that resulted in a premature stop codon at the 5′ end of *2crr* (TAC to TAG), along with downstream deletion of a 562-bp region within *2crr* (Fig. 5A). Similarly, removal of a 1,299-bp region within the *glgA* gene of Lpc-37 was confirmed by sequencing of the *glgA* PCR amplicon from the mutants (Fig. 5B). No apparent phenotypic change was observed in the Δ*2crr* mutant (NCK2775) compared to the parent ATCC 33323, although the ortholog of 2CRR_Lgas0710 in *L. acidophilus* NCFM is essential for bile tolerance *in vitro* (59). As expected, an iodine staining assay for intracellular glycogen detection in *L. paracasei* showed a deficiency of glycogen accumulation in the Δ*glgA* mutant compared to the parent strain (Fig. 5B). This result indicated that *glgA* inactivation disrupted the glycogen biosynthetic pathway in the mutant and consequently its inability to synthesize intracellular glycogen. Overall, the editing efficacy of the pLbCas9^N as demonstrated in *L. gasseri* and *L. paracasei* is promising for the exploitation of the system in other lactobacilli.

Conclusion. In this study, we developed a Cas9^N-based genome editing system for programmable genome engineering in *L. acidophilus* and demonstrated the portability of the system in two other *Lactobacillus* species, namely, *L. gasseri* and *L. paracasei*. Overall, the observed editing efficiencies (up to 100%) and diverse editing outcomes highlighted the robustness and versatility of the pLbCas9^N system, including (i) flexible site-specific manipulation at different chromosomal loci, (ii) a varying deletion size range, and (iii) a customizable repair template design for multiple concurrent mutations.

Recovery of deletion mutants can be achieved within 1 week posttransformation, thus significantly accelerating precise gene deletion throughput for functional studies of probiotic mechanisms compared to conventional double-crossover recombination. In some instances where edited cells were present together with unedited cells, a subsequent purification step was applied to the mixed-genotype culture to recover pure mutant populations. The instability of pLbCas9^N editing plasmids in the absence of antibiotic selective pressure enabled efficient curing of the plasmid after editing and generation of iterative genome manipulations in the same host. Aside from the broad-host-range replicon and the modular design of the pLbCas9^N system, the portability of the system is also conferred by its compatibility in hosts with intact or degenerate CRISPR-Cas systems (e.g., *L. acidophilus* and *L. paracasei*).

The GRAS (generally regarded as safe) status of most lactobacillus species has led to the recent emergence of various *Lactobacillus* strains as attractive candidates for engineered biotherapeutics. Hence, the pLbCas9^N system represents a valuable tool for precise chromosomal manipulation of genes and pathways of interests and for exploiting highly expressed chromosomal regions (e.g., downstream of the constitutive highly expressed *pgm* gene) for gene insertion to achieve high and stable coexpression of target genes without relying on conventional heterologous plasmid expression. The tool and approaches presented in this work will serve as additional modalities for the timely development of *L. acidophilus*, and potentially other health-promoting *Lactobacillus* species, as next-generation mucosal vaccine and biotherapeutic delivery vehicles.

MATERIALS AND METHODS

Bacterial strains and growth conditions. The strains and plasmids used in this study are listed in Table 1. *E. coli* transformants were selected and propagated at 30°C in Luria-Bertani (LB) medium (Difco Laboratories, Detroit, MI) supplemented with 15 μg/ml of Cm (Sigma, St. Louis, MO). *Lactobacillus* strains were propagated in MRS broth (Difco) statically under ambient atmospheric conditions or on MRS agar (1.5% [wt/vol]; Difco) under anaerobic conditions at 37°C. *Lactobacillus* plasmid transformants were selected in the presence of 5 μg/ml of Cm for both *L. acidophilus* and *L. paracasei* and 7.5 μg/ml for *L. gasseri*.

DNA manipulations and transformation. Genomic DNA was isolated using a *Quick*-DNA fungal/bacterial kit (Zymo Research, Irvine, CA) according to the manufacturer's protocol. Plasmid DNA from *E. coli* was purified using a QIAprep spin miniprep kit (Qiagen Inc., Valencia, CA). Restriction enzymes and a Quick dephosphorylation kit (New England Biolabs [NEB], Ipswich, MA) were used per the manufacturer's instructions. DNA ligation was performed using Instant Sticky-end Ligase master mix (NEB). DNA fragments for plasmid construction were assembled using NEBuilder HiFi DNA assembly master mix (NEB) based on the manufacturer's recommendations. Oligonucleotide primers for PCR and Sanger sequencing were synthesized by Integrated DNA Technologies (Coralville, IA). Gene fragments and sgRNA sequences were synthesized by Genewiz (South Plainfield, NJ). For cloning and Sanger sequencing purposes, PCR amplicons were generated using Q5 Hot Start high-fidelity 2$\times$ master mix (NEB) according to the supplier's instructions. Routine PCR amplifications for screening of transformants were performed by using standard protocols and Choice-Taq Blue DNA polymerase (Thomas Scientific, Swedesboro, NJ). PCR amplicons were gel-purified using Monarch DNA gel extraction kits (NEB) followed by Monarch PCR and DNA cleanup kits (NEB), or with E-Gel CloneWell II agarose gels (Thermo Fisher Scientific), followed by further purification of the recovered products using Monarch PCR and DNA cleanup kits. Sanger sequencing to verify sequence integrity of PCR amplicons and plasmid constructs was performed by Genewiz.

E. coli chemically competent cells were prepared and transformed based on procedures previously described by Hanahan (60). Transformed cells were recovered with SOC medium (Corning Mediatech, Manassas, VA) at 30°C with aeration for 3 h prior to plating on selective medium and incubation at 30°C. *L. acidophilus*, *L. gasseri*, and *L. paracasei* cells were prepared for electroporation as described previously (11). Prepared cell aliquots (200 μl) were electroporated with 1 to 2 μg of each pLbCas9^N plasmid construct, and transformed cells were recovered in 1.8 ml of MRS medium overnight at 37°C, followed by dilution and plating on selective medium.

Construction of a lactobacillus SpyCas9^{D10A}-expressing vector for targeted genome editing. For construction of a lactobacillus Cas9 nickase-expressing vector, the SpyCas9^{D10A} sequence along with its ribosomal binding site was amplified from pCas9(D10A) (Table 2), a gift from Xiao Wang (Addgene plasmid 74495; RRID, Addgene_74495) (32), with PstI restriction sites added on both ends of the SpyCas9^{D10A} amplicons. The purified 4.1-kb amplicon was digested with PstI and ligated with similarly digested and dephosphorylated pTRK687 vector. The ligation mix was transformed into *E. coli* cloning hosts, and transformants were selected on LB plates containing Cm. The resulting 7.1-kb Cas9 nickase expressing vector, pLbCas9^N or pTRK1203, was maintained in *E. coli* MC1061 cloning host, and the stability of the *cas9*^{N} insert was verified by restriction digest analysis and Sanger sequencing.

Design and construction of pLbCas9^N-based editing plasmids. To design sgRNA for targeted gene deletions and gene insertion, SpyCas9 target sites at each of the targeted editing locus were scanned and predicted using the CRISPy-web server (61). For each SpyCas9 target candidate, the seed region of the guide sequence was manually scanned along the genome using Geneious to verify the absence of potential off-target matches. The 19- to 20-nucleotide guide region along with the gRNA scaffold and termination signal was designed according to a protocol by Mali (https://media.addgene.org/cms/files/hCRISPR_gRNA_Synthesis.pdf). The predicted promoter sequence for the housekeeping *tuf* gene of each respective *Lactobacillus* strain (NCFM, ATCC 33323, or Lpc-37), along with the target-specific sgRNA, and an editing/repair template consisting of 1-kb homologous arms flanking the target site were designed as a single gene block with added BglII restriction sites on both ends and synthesized by Genewiz. Each gene block was digested with BglII and ligated into similarly digested and dephosphorylated pLbCas9^N vector.

For chromosomal insertion of the mCherry-encoding gene between the stop codon of *pgm* and its transcriptional terminator in *L. acidophilus*, the mCherry amino acid sequence was obtained from pRSET-B mCherry (62) and the corresponding 711-bp gene sequence, codon optimized for *L. acidophilus* NCFM, was generated using the web-based JCat (Java Codon Adaptation Tool) (63). The P*tuf*-sgRNA, a partial sequence of the repair template (homologous to the 1.5-kb flanking region downstream of the insertion site), and the codon-optimized mCherry gene with ribosomal-binding region of *pgm* added at the 5′ end were synthesized as a gene block and amplified with the primer pair lac_pgmCy-1F/lac_pgmCy-1R (Table 2), while the remaining portion of the repair template (homologous to the 1.5-kb flanking region upstream of insertion site) was amplified from the chromosome with the primer pair lac_pgmCy-2F/lac_pgmCy-2R. Both fragments were subsequently assembled into BglII-digested pLbCas9^N using NEBuilder HiFi DNA assembly master mix. Ligation and assembly mixes were transformed into *E. coli* MC1061 cells, and transformants were recovered on LB supplemented with Cm at 30°C incubation. The sequence integrity of all plasmid inserts was verified by restriction digest analysis and Sanger sequencing prior to transformation into *Lactobacillus* hosts.

Isolation of edited mutants and plasmid curing. Transformants of pLbCas9^N editing plasmids were screened for targeted deletions or insertion by colony PCR with chromosomal-specific primers flanking the regions homologous to the editing templates (Table 2). Pure population of edited cells were purified by streaking on MRS plates with Cm and PCR analysis. The absence of wild-type cells was confirmed by PCR with one of the primers that annealed specifically to the deleted region and thus produced amplicons only in the presence of cells retaining wild-type genotypes. For plasmid curing, pure mutant strains were propagated in MRS broth without Cm, and overnight cultures (ca. 10 generations) were plated to obtain isolated colonies. Selected colonies were replica plated on MRS and MRS with Cm plates. Sensitivity to Cm exhibited by colonies indicated loss of the pLbCas9^N editing plasmids, which was further confirmed by establishing the absence of PCR amplicons using primers specific to the pLbCas9^N backbone (Table 2) (expected amplicon size of 960 bp).

Carbohydrate growth experiments and intracellular glycogen assays. For carbohydrate growth experiments, *L. acidophilus* NCFM and its mutant derivatives NCK2773 (Δ*rafE*) and NCK2774 (Δ*lacS*) were grown in semidefined medium (64) (SDM) with glucose substituted for raffinose or lactose. Stationary-phase cultures grown in MRS broth (16 h of growth) were inoculated at 1% (vol/vol) into 96-well microplate wells (Corning Costar, Corning, NY) in triplicate, each containing 200 μl of SDM supplemented with 1% of the carbohydrate. Microplates were sealed with clear Thermalseal film (ISC Bioexpress, Kaysville, UT), incubated at 37°C in a Fluostar Optima microplate reader (BMG Labtech, Cary, NC), and optical density of the cells was monitored at 600 nm for 48 h. Qualitative detection of intracellular glycogen in *L. paracasei* Lpc-37 and NCK2776 (Δ*glgA*) mutant strains by iodine-staining method was performed as described previously (65).

SEM. *L. acidophilus* NCFM and NCK2676 (Δ*ltaS*) strains were grown in MRS medium to an optical density at 600 nm (OD_{600}) of 0.6 to 0.8 (mid-log phase) and pelleted by centrifugation at 3,166 $\times$ *g* at room temperature. Cell pellets were resuspended in a fresh 1:1 (vol/vol) fixative mixture containing 3% glutaraldehyde in 0.1 M cacodylate (pH 5.5) and stored at 4°C until processed. Samples were processed for SEM by the Center for Electron Microscopy (CEM) at North Carolina State University and viewed with a JEOL JEM-5900LV SEM at 15 kV. Images were acquired digitally using a JEOL digital scan generator at a resolution of 1,280 by 960 pixels.

Fluorescence microscopy. *L. acidophilus* NCFM and NCK2777 NCFM::mCherry gene integrant strains were grown in MRS broth at 37°C under ambient atmosphere conditions for 16 h. Aliquots (8 μl) of cultures were placed on microscope glass slides, and mCherry fluorescence was visualized at a magnification of $\times$40 under a Nikon Eclipse E600 microscope equipped with an AT-TRITC/Cy3/TagRFP/Alexa Fluor 546 filter set (excitation at 540 nm, emission at 605 nm).

Whole-genome sequencing of *L. acidophilus* mutants. Overnight cultures grown in MRS medium (30 ml) were harvested, and frozen cell pellets were submitted to the High-Throughput Sequencing and Genotyping Unit of the Roy J. Carver Biotechnology Center at the University of Illinois for genomic extraction, whole-genome sequencing, and genome assembly. Genomic DNA was extracted using the MasterPure Gram Positive DNA purification kit (Lucigen, Middleton, WI). For Illumina MiSeq paired-end sequencing, shotgun genomic libraries were prepared with the Hyper Library construction kit from Kapa Biosystems (Roche). The library pool was quantitated by qPCR and sequenced on one ISeq flow cell for 151 cycles from each end of the fragments, which yielded paired-end read lengths of 250 nucleotides (nt). Fastq files were generated and demultiplexed with the bcl2fastq v2.20 conversion software (Illumina), and adapters were trimmed from the 3′ ends of the reads. For Oxford Nanopore sequencing,

the genome DNA samples were converted into individual barcoded libraries with the NBD104 (barcoding) and LSK109 (library) kits from Oxford Nanopore (Oxford, UK).

The libraries were pooled and sequenced on two SpotON R10.1 RevD FLO-MIN106 flow cells for 48 h, using a GridIONx5 sequencer. Base calling was performed with Guppy (ver. 3.2.6), and demultiplexing and adapter removal were performed with Porechop (ver. 0.2.3) (66). For hybrid assembly of the genome sequences, Illumina MiSeq and Oxford Nanopore long reads were checked for quality prior to and after trimming using FastQC v0.11.8 (67). MiSeq reads were trimmed using Trimmomatic v0.38 (68) with parameters set to ILLUMINACLIP:TruSeq3-PE-2.fa:2:15:10 LEADING:28 TRAILING:28 MINLEN:30, retaining reads longer than 30 bp. Long reads were adapter trimmed with Porechop v0.2.3 (66) and length filtered to a minimum of 1 kb with seqtk v1.3 (69). Unicycler v0.4.8 (70) assembled the trimmed MiSeq and uncorrected Oxford Nanopore reads in a hybrid assembly using the default "normal" mode. Within Unicycler, the MiSeq reads were assembled with SPAdes v3.11.1 (71), and the resulting long-anchor contigs were assembled together with the Oxford Nanopore reads by an optimized version of miniasm (72) and Racon v0.5.0 (73). Pilon v1.22 (74) was used within Unicycler to iteratively polish the assembly with the MiSeq reads. The circularized genome assemblies were annotated using Prokka v1.14.6 (75) with parameters set for *L. acidophilus*. Assemblies were evaluated for completeness using BUSCO v3.0.1 (76) with the appropriate bacterial lineage.

To compare the genome sequences of the NCFM mutants (Δ*rafE*, Δ*lacS*, and Δ*ltaS*) with the parent strain, sequencing reads from Illumina MiSeq (average, 2.3 million paired-end reads/sample) and Oxford Nanopore (average, 2 billion bases/sample) were mapped to NCFM reference genome (NC_006814) using Bowtie2 mapper (77) within Geneious software v11.1.15 with default settings. Assembled genomes of the NCFM mutants were aligned with the reference genome using Mauve plugin in Geneious, with the progressiveMauve alignment algorithm (78).

Data availability. Genome sequence data for the *L. acidophilus* NCFM Δ*rafE* (NCK2773), Δ*lacS* (NCK2774), and Δ*ltaS* (NCK2676) mutants have been deposited in the NCBI Sequence Read Archive (SRA) database under BioProject ID PRJNA681755 (BioSample accession numbers SAMN16967693 to SAMN16967695).

ACKNOWLEDGMENTS

This work was supported in part by the North Carolina Agricultural Foundation and DuPont Nutrition & Health USA, Inc.

We thank Valerie Lapham at the NCSU College of Agricultural and Life Sciences Center for Electron Microscopy for assistance in SEM imaging. We also express our gratitude to Alvaro Hernandez and Chris Wright at the University of Illinois at Urbana-Champaign (UIUC) Roy Carver Biotechnology Center for genome sequencing services, and Christopher Fields and Kimberly Walden at the UIUC Roy Carver Biotechnology Center and High-Performance Biological Computing for bioinformatics service and expertise in genome assembly.

REFERENCES

1. Morovic W, Hibberd AA, Zabel B, Barrangou R, Stahl B. 2016. Genotyping by PCR and high-throughput sequencing of commercial probiotic products reveals composition biases. Front Microbiol 7:1747. https://doi.org/10.3389/fmicb.2016.01747.
2. Bull MJ, Jolley KA, Bray JE, Aerts M, Vandamme P, Maiden MC, Marchesi JR, Mahenthiralingam E. 2014. The domestication of the probiotic bacterium *Lactobacillus acidophilus*. Sci Rep 4:7202. https://doi.org/10.1038/srep07202.
3. Gilliland SE, Speck ML, Morgan CG. 1975. Detection of *Lactobacillus acidophilus* in feces of humans, pigs, and chickens. Appl Microbiol 30:541–545. https://doi.org/10.1128/AM.30.4.541-545.1975.
4. Leyer GJ, Li S, Mubasher ME, Reifer C, Ouwehand AC. 2009. Probiotic effects on cold and influenza-like symptom incidence and duration in children. Pediatrics 124:e172–e179. https://doi.org/10.1542/peds.2008-2666.
5. Rousseaux C, Thuru X, Gelot A, Barnich N, Neut C, Dubuquoy L, Dubuquoy C, Merour E, Geboes K, Chamaillard M, Ouwehand A, Leyer G, Carcano D, Colombel JF, Ardid D, Desreumaux P. 2007. *Lactobacillus acidophilus* modulates intestinal pain and induces opioid and cannabinoid receptors. Nat Med 13:35–37. https://doi.org/10.1038/nm1521.
6. Konstantinov SR, Smidt H, de Vos WM, Bruijns SC, Singh SK, Valence F, Molle D, Lortal S, Altermann E, Klaenhammer TR, van Kooyk Y. 2008. S layer protein A of *Lactobacillus acidophilus* NCFM regulates immature dendritic cell and T cell functions. Proc Natl Acad Sci U S A 105:19474–19479. https://doi.org/10.1073/pnas.0810305105.
7. Mohamadzadeh M, Duong T, Sandwick SJ, Hoover T, Klaenhammer TR. 2009. Dendritic cell targeting of *Bacillus anthracis* protective antigen expressed by *Lactobacillus acidophilus* protects mice from lethal challenge. Proc Natl Acad Sci U S A 106:4331–4336. https://doi.org/10.1073/pnas.0900029106.
8. Kajikawa A, Zhang L, Long J, Nordone S, Stoeker L, LaVoy A, Bumgardner S, Klaenhammer T, Dean G. 2012. Construction and immunological evaluation of dual cell surface display of HIV-1 Gag and *Salmonella enterica* serovar Typhimurium FliC in *Lactobacillus acidophilus* for vaccine delivery. Clin Vaccine Immunol 19:1374–1381. https://doi.org/10.1128/CVI.00049-12.
9. Leenhouts K, Buist G, Bolhuis A, ten Berge A, Kiel J, Mierau I, Dabrowska M, Venema G, Kok J. 1996. A general system for generating unlabelled gene replacements in bacterial chromosomes. Mol Gen Genet 253:217–224. https://doi.org/10.1007/s004380050315.
10. Russell WM, Klaenhammer TR. 2001. Efficient system for directed integration into the *Lactobacillus acidophilus* and *Lactobacillus gasseri* chromosomes via homologous recombination. Appl Environ Microbiol 67:4361–4364. https://doi.org/10.1128/aem.67.9.4361-4364.2001.
11. Goh YJ, Azcarate-Peril MA, O'Flaherty S, Durmaz E, Valence F, Jardin J, Lortal S, Klaenhammer TR. 2009. Development and application of a *upp*-based counterselective gene replacement system for the study of the S-layer protein SlpX of *Lactobacillus acidophilus* NCFM. Appl Environ Microbiol 75:3093–3105. https://doi.org/10.1128/AEM.02502-08.
12. Douglas GL, Goh YJ, Klaenhammer TR. 2011. Integrative food grade expression system for lactic acid bacteria. Methods Mol Biol 765:373–387. https://doi.org/10.1007/978-1-61779-197-0_22.
13. Ishino Y, Shinagawa H, Makino K, Amemura M, Nakata A. 1987. Nucleotide sequence of the *iap* gene, responsible for alkaline phosphatase isozyme conversion in *Escherichia coli*, and identification of the gene product. J Bacteriol 169:5429–5433. https://doi.org/10.1128/jb.169.12.5429-5433.1987.

14. Mojica FJ, Diez-Villasenor C, Soria E, Juez G. 2000. Biological significance of a family of regularly spaced repeats in the genomes of Archaea, Bacteria and mitochondria. Mol Microbiol 36:244–246. https://doi.org/10.1046/j.1365-2958.2000.01838.x.
15. Jinek M, Chylinski K, Fonfara I, Hauer M, Doudna JA, Charpentier E. 2012. A programmable dual-RNA-guided DNA endonuclease in adaptive bacterial immunity. Science 337:816–821. https://doi.org/10.1126/science.1225829.
16. Gasiunas G, Barrangou R, Horvath P, Siksnys V. 2012. Cas9-crRNA ribonucleoprotein complex mediates specific DNA cleavage for adaptive immunity in bacteria. Proc Natl Acad Sci U S A 109:E2579–E2586. https://doi.org/10.1073/pnas.1208507109.
17. Cong L, Ran FA, Cox D, Lin S, Barretto R, Habib N, Hsu PD, Wu X, Jiang W, Marraffini LA, Zhang F. 2013. Multiplex genome engineering using CRISPR/Cas systems. Science 339:819–823. https://doi.org/10.1126/science.1231143.
18. Mali P, Yang L, Esvelt KM, Aach J, Guell M, DiCarlo JE, Norville JE, Church GM. 2013. RNA-guided human genome engineering via Cas9. Science 339:823–826. https://doi.org/10.1126/science.1232033.
19. Wilkinson R, Wiedenheft B. 2014. A CRISPR method for genome engineering. F1000Prime Rep 6:3. https://doi.org/10.12703/P6-3.
20. Barrangou R, Horvath P. 2017. A decade of discovery: CRISPR functions and applications. Nat Microbiol 2:17092. https://doi.org/10.1038/nmicrobiol.2017.92.
21. Knott GJ, Doudna JA. 2018. CRISPR-Cas guides the future of genetic engineering. Science 361:866–869. https://doi.org/10.1126/science.aat5011.
22. Ramachandran G, Bikard D. 2019. Editing the microbiome the CRISPR way. Philos Trans R Soc Lond B Biol Sci 374:20180103. https://doi.org/10.1098/rstb.2018.0103.
23. Barrangou R, Fremaux C, Deveau H, Richards M, Boyaval P, Moineau S, Romero DA, Horvath P. 2007. CRISPR provides acquired resistance against viruses in prokaryotes. Science 315:1709–1712. https://doi.org/10.1126/science.1138140.
24. Westra ER, Buckling A, Fineran PC. 2014. CRISPR-Cas systems: beyond adaptive immunity. Nat Rev Microbiol 12:317–326. https://doi.org/10.1038/nrmicro3241.
25. Horvath P, Romero DA, Coute-Monvoisin AC, Richards M, Deveau H, Moineau S, Boyaval P, Fremaux C, Barrangou R. 2008. Diversity, activity, and evolution of CRISPR loci in *Streptococcus thermophilus*. J Bacteriol 190:1401–1412. https://doi.org/10.1128/JB.01415-07.
26. Jinek M, East A, Cheng A, Lin S, Ma E, Doudna J. 2013. RNA-programmed genome editing in human cells. Elife 2:e00471. https://doi.org/10.7554/eLife.00471.
27. Jiang W, Bikard D, Cox D, Zhang F, Marraffini LA. 2013. RNA-guided editing of bacterial genomes using CRISPR-Cas systems. Nat Biotechnol 31:233–239. https://doi.org/10.1038/nbt.2508.
28. Selle K, Barrangou R. 2015. Harnessing CRISPR-Cas systems for bacterial genome editing. Trends Microbiol 23:225–232. https://doi.org/10.1016/j.tim.2015.01.008.
29. Cui L, Bikard D. 2016. Consequences of Cas9 cleavage in the chromosome of *Escherichia coli*. Nucleic Acids Res 44:4243–4251. https://doi.org/10.1093/nar/gkw223.
30. Jiang Y, Chen B, Duan C, Sun B, Yang J, Yang S. 2015. Multigene editing in the *Escherichia coli* genome via the CRISPR-Cas9 system. Appl Environ Microbiol 81:2506–2514. https://doi.org/10.1128/AEM.04023-14.
31. Reisch CR, Prather KL. 2015. The no-SCAR (Scarless Cas9 Assisted Recombineering) system for genome editing in *Escherichia coli*. Sci Rep 5:15096. https://doi.org/10.1038/srep15096.
32. Standage-Beier K, Zhang Q, Wang X. 2015. Targeted large-scale deletion of bacterial genomes using CRISPR-nickases. ACS Synth Biol 4:1217–1225. https://doi.org/10.1021/acssynbio.5b00132.
33. Westbrook AW, Moo-Young M, Chou CP. 2016. Development of a CRISPR-Cas9 tool kit for comprehensive engineering of *Bacillus subtilis*. Appl Environ Microbiol 82:4876–4895. https://doi.org/10.1128/AEM.01159-16.
34. Li K, Cai D, Wang Z, He Z, Chen S. 2018. Development of an efficient genome editing tool in *Bacillus licheniformis* using CRISPR-Cas9 nickase. Appl Environ Microbiol 84:e02608-17. https://doi.org/10.1128/AEM.02608-17.
35. Liu D, Huang C, Guo J, Zhang P, Chen T, Wang Z, Zhao X. 2019. Development and characterization of a CRISPR/Cas9n-based multiplex genome editing system for *Bacillus subtilis*. Biotechnol Biofuels 12:197. https://doi.org/10.1186/s13068-019-1537-1.
36. Guo T, Xin Y, Zhang Y, Gu X, Kong J. 2019. A rapid and versatile tool for genomic engineering in *Lactococcus lactis*. Microb Cell Fact 18:22. https://doi.org/10.1186/s12934-019-1075-3.
37. Wang Y, Zhang ZT, Seo SO, Choi K, Lu T, Jin YS, Blaschek HP. 2015. Markerless chromosomal gene deletion in *Clostridium beijerinckii* using CRISPR/Cas9 system. J Biotechnol 200:1–5. https://doi.org/10.1016/j.jbiotec.2015.02.005.
38. Xu T, Li Y, Shi Z, Hemme CL, Li Y, Zhu Y, Van Nostrand JD, He Z, Zhou J. 2015. Efficient genome editing in *Clostridium cellulolyticum* via CRISPR-Cas9 nickase. Appl Environ Microbiol 81:4423–4431. https://doi.org/10.1128/AEM.00873-15.
39. Liu J, Wang Y, Lu Y, Zheng P, Sun J, Ma Y. 2017. Development of a CRISPR/Cas9 genome editing toolbox for *Corynebacterium glutamicum*. Microb Cell Fact 16:205. https://doi.org/10.1186/s12934-017-0815-5.
40. Cobb RE, Wang Y, Zhao H. 2015. High-efficiency multiplex genome editing of *Streptomyces* species using an engineered CRISPR/Cas system. ACS Synth Biol 4:723–728. https://doi.org/10.1021/sb500351f.
41. Huang H, Zheng G, Jiang W, Hu H, Lu Y. 2015. One-step high-efficiency CRISPR/Cas9-mediated genome editing in *Streptomyces*. Acta Biochim Biophys Sin (Shanghai) 47:231–243. https://doi.org/10.1093/abbs/gmv007.
42. Tong Y, Charusanti P, Zhang L, Weber T, Lee SY. 2015. CRISPR-Cas9 based engineering of actinomycetal genomes. ACS Synth Biol 4:1020–1029. https://doi.org/10.1021/acssynbio.5b00038.
43. Mougiakos I, Bosma EF, de Vos WM, van Kranenburg R, van der Oost J. 2016. Next generation prokaryotic engineering: the CRISPR-Cas toolkit. Trends Biotechnol 34:575–587. https://doi.org/10.1016/j.tibtech.2016.02.004.
44. Oh JH, van Pijkeren JP. 2014. CRISPR-Cas9-assisted recombineering in *Lactobacillus reuteri*. Nucleic Acids Res 42:e131. https://doi.org/10.1093/nar/gku623.
45. Leenay RT, Vento JM, Shah M, Martino ME, Leulier F, Beisel CL. 2018. Genome editing with CRISPR-Cas9 in *Lactobacillus plantarum* revealed that editing outcomes can vary across strains and between methods. Biotechnol J 14:e1700583. https://doi.org/10.1002/biot.201700583.
46. Zhou D, Jiang Z, Pang Q, Zhu Y, Wang Q, Qi Q. 2019. CRISPR/Cas9-assisted seamless genome editing in *Lactobacillus plantarum* and its application in *N*-acetylglucosamine production. Appl Environ Microbiol 85:e01367-19. https://doi.org/10.1128/AEM.01367-19.
47. Song X, Huang H, Xiong Z, Ai L, Yang S. 2017. CRISPR-Cas9$^{(D10A)}$ nickase-assisted genome editing in *Lactobacillus casei*. Appl Environ Microbiol 83:e01259-17. https://doi.org/10.1128/AEM.01259-17.
48. Huang H, Song X, Yang S. 2019. Development of a RecE/T-assisted CRISPR-Cas9 toolbox for *Lactobacillus*. Biotechnol J 14:e1800690. https://doi.org/10.1002/biot.201800690.
49. Crawley AB, Henriksen ED, Stout E, Brandt K, Barrangou R. 2018. Characterizing the activity of abundant, diverse and active CRISPR-Cas systems in lactobacilli. Sci Rep 8:11544. https://doi.org/10.1038/s41598-018-29746-3.
50. Hidalgo-Cantabrana C, Goh YJ, Pan M, Sanozky-Dawes R, Barrangou R. 2019. Genome editing using the endogenous type I CRISPR-Cas system in *Lactobacillus crispatus*. Proc Natl Acad Sci U S A 116:15774–15783. https://doi.org/10.1073/pnas.1905421116.
51. Altermann E, Russell WM, Azcarate-Peril MA, Barrangou R, Buck BL, McAuliffe O, Souther N, Dobson A, Duong T, Callanan M, Lick S, Hamrick A, Cano R, Klaenhammer TR. 2005. Complete genome sequence of the probiotic lactic acid bacterium *Lactobacillus acidophilus* NCFM. Proc Natl Acad Sci U S A 102:3906–3912. https://doi.org/10.1073/pnas.0409188102.
52. Kok J, van der Vossen JM, Venema G. 1984. Construction of plasmid cloning vectors for lactic streptococci which also replicate in *Bacillus subtilis* and *Escherichia coli*. Appl Environ Microbiol 48:726–731. https://doi.org/10.1128/AEM.48.4.726-731.1984.
53. De Vos WM. 1987. Gene cloning and expression in lactic streptococci. FEMS Microbiol Lett 46:281–295. https://doi.org/10.1016/0378-1097(87)90113-3.
54. Sturino JM, Klaenhammer TR. 2002. Expression of antisense RNA targeted against *Streptococcus thermophilus* bacteriophages. Appl Environ Microbiol 68:588–596. https://doi.org/10.1128/aem.68.2.588-596.2002.
55. Djordjevic G, Bojovic B, Miladinov N, Topisirovic L. 1997. Cloning and molecular analysis of promoter-like sequences isolated from the chromosomal DNA of *Lactobacillus acidophilus* ATCC 4356. Can J Microbiol 43:61–69. https://doi.org/10.1139/m97-009.
56. Selle K, Goh YJ, Johnson BR, O'Flaherty S, Andersen JM, Barrangou R, Klaenhammer TR. 2017. Deletion of lipoteichoic acid synthase impacts expression of genes encoding cell surface proteins in *Lactobacillus acidophilus*. Front Microbiol 8:553. https://doi.org/10.3389/fmicb.2017.00553.
57. Lauer E, Kandler O. 1980. *Lactobacillus gasseri* sp. nov., a new species of the subgenus *Thermobacterium*. Zentralbl Bakteriol Mikrobiol Hyg Abt 1 Orig C 1:75–78.
58. Azcarate-Peril MA, Altermann E, Goh YJ, Tallon R, Sanozky-Dawes RB, Pfeiler EA, O'Flaherty S, Buck BL, Dobson A, Duong T, Miller MJ, Barrangou R, Klaenhammer TR. 2008. Analysis of the genome sequence of

Lactobacillus gasseri ATCC 33323 reveals the molecular basis of an autochthonous intestinal organism. Appl Environ Microbiol 74:4610–4625. https://doi.org/10.1128/AEM.00054-08.
59. Pfeiler EA, Azcarate-Peril MA, Klaenhammer TR. 2007. Characterization of a novel bile-inducible operon encoding a two-component regulatory system in *Lactobacillus acidophilus*. J Bacteriol 189:4624–4634. https://doi.org/10.1128/JB.00337-07.
60. Hanahan D. 1985. Techniques for transformation of *E. coli*, p 109–135. *In* Glover DM (ed), DNA cloning: a practical approach, vol 1. IRL Press Ltd., Oxford, England.
61. Blin K, Pedersen LE, Weber T, Lee SY. 2016. CRISPy-web: an online resource to design sgRNAs for CRISPR applications. Synth Syst Biotechnol 1:118–121. https://doi.org/10.1016/j.synbio.2016.01.003.
62. Sarabipour S, King C, Hristova K. 2014. Uninduced high-yield bacterial expression of fluorescent proteins. Anal Biochem 449:155–157. https://doi.org/10.1016/j.ab.2013.12.027.
63. Grote A, Hiller K, Scheer M, Munch R, Nortemann B, Hempel DC, Jahn D. 2005. JCat: a novel tool to adapt codon usage of a target gene to its potential expression host. Nucleic Acids Res 33:W526–W531. https://doi.org/10.1093/nar/gki376.
64. Kimmel SA, Roberts RF. 1998. Development of a growth medium suitable for exopolysaccharide production by *Lactobacillus delbrueckii* ssp. *bulgaricus* RR. Int J Food Microbiol 40:87–92. https://doi.org/10.1016/s0168-1605(98)00023-3.
65. Goh YJ, Klaenhammer TR. 2013. A functional glycogen biosynthesis pathway in *Lactobacillus acidophilus*: expression and analysis of the *glg* operon. Mol Microbiol 89:1187–1200. https://doi.org/10.1111/mmi.12338.
66. Wick RR. 2017. Porechop. https://github.com/rrwick/Porechop.
67. Andrews S. 2010. FastQC: a quality control tool for high throughput sequence data http://www.bioinformatics.babraham.ac.uk/projects/fastqc/.
68. Bolger AM, Lohse M, Usadel B. 2014. Trimmomatic: a flexible trimmer for Illumina sequence data. Bioinformatics 30:2114–2120. https://doi.org/10.1093/bioinformatics/btu170.
69. Li H. 2018. seqtk. https://github.com/lh3/seqtk.
70. Wick RR, Judd LM, Gorrie CL, Holt KE. 2017. Unicycler: resolving bacterial genome assemblies from short and long sequencing reads. PLoS Comput Biol 13:e1005595. https://doi.org/10.1371/journal.pcbi.1005595.
71. Bankevich A, Nurk S, Antipov D, Gurevich AA, Dvorkin M, Kulikov AS, Lesin VM, Nikolenko SI, Pham S, Prjibelski AD, Pyshkin AV, Sirotkin AV, Vyahhi N, Tesler G, Alekseyev MA, Pevzner PA. 2012. SPAdes: a new genome assembly algorithm and its applications to single-cell sequencing. J Comput Biol 19:455–477. https://doi.org/10.1089/cmb.2012.0021.
72. Li H. 2016. Minimap and miniasm: fast mapping and *de novo* assembly for noisy long sequences. Bioinformatics 32:2103–2110. https://doi.org/10.1093/bioinformatics/btw152.
73. Vaser R, Sovic I, Nagarajan N, Sikic M. 2017. Fast and accurate de novo genome assembly from long uncorrected reads. Genome Res 27:737–746. https://doi.org/10.1101/gr.214270.116.
74. Walker BJ, Abeel T, Shea T, Priest M, Abouelliel A, Sakthikumar S, Cuomo CA, Zeng Q, Wortman J, Young SK, Earl AM. 2014. Pilon: an integrated tool for comprehensive microbial variant detection and genome assembly improvement. PLoS One 9:e112963. https://doi.org/10.1371/journal.pone.0112963.
75. Seemann T. 2014. Prokka: rapid prokaryotic genome annotation. Bioinformatics 30:2068–2069. https://doi.org/10.1093/bioinformatics/btu153.
76. Waterhouse RM, Seppey M, Simao FA, Manni M, Ioannidis P, Klioutchnikov G, Kriventseva EV, Zdobnov EM. 2018. BUSCO applications from quality assessments to gene prediction and phylogenomics. Mol Biol Evol 35:543–548. https://doi.org/10.1093/molbev/msx319.
77. Langmead B, Salzberg SL. 2012. Fast gapped-read alignment with Bowtie 2. Nat Methods 9:357–359. https://doi.org/10.1038/nmeth.1923.
78. Darling AC, Mau B, Blattner FR, Perna NT. 2004. Mauve: multiple alignment of conserved genomic sequence with rearrangements. Genome Res 14:1394–1403. https://doi.org/10.1101/gr.2289704.
79. Barefoot SF, Klaenhammer TR. 1983. Detection and activity of lactacin B, a bacteriocin produced by *Lactobacillus acidophilus*. Appl Environ Microbiol 45:1808–1815. https://doi.org/10.1128/AEM.45.6.1808-1815.1983.
80. Casadaban MJ, Cohen SN. 1980. Analysis of gene control signals by DNA fusion and cloning in *Escherichia coli*. J Mol Biol 138:179–207. https://doi.org/10.1016/0022-2836(80)90283-1.